17th World Conference on Earthquake Engineering, 17WCEE
Sendai, Japan - September 13th to 18th 2020

ON THE APPLICABILITY OF A MULTIPLE SHEAR SPRINGS ALGEBRAIC MODEL FOR RESPONSE HISTORY ANALYSES OF FIBER-REINFORCED BEARINGS BASE-ISOLATED BUILDINGS

A. Calabrese[(1)], N. Vaiana[(2)], D. Losanno[(3)], S. Galano[(4)]

[(1)] *Department of Structures for Engineering and Architecture, University of Naples Federico II, via Claudio, 21, 80124, Naples, Italy, nicolo.vaiana@unina.it*
[(2)] *Department of Civil Engineering and Construction Engineering Management, University of California State Long Beach, 1250 Bellflower Blvd., Long Beach, CA, 90840, Andrea.Calabrese@csulb.edu*
[(3)] *Department of Structures for Engineering and Architecture, University of Naples Federico II, via Claudio, 21, 80124, Naples, Italy, daniele.losanno@unina.it –*
Construction Technologies Institute, National Research Council of Italy, San Giuliano Milanese, Milano, Italy
[(4)] *Department of Civil Engineering and Construction Engineering Management, University of California State Long Beach, 1250 Bellflower Blvd., Long Beach, CA, 90840, Simone.Galano@csulb.edu*
Department of Structures for Engineering and Architecture, University of Naples Federico II, via Claudio, 21, 80124, Naples, Italy

Abstract

In this paper, a novel phenomenological model describing the 2D hysteresis response of base-isolated buildings on fiber-reinforced bearings (FRBs) is presented. The proposed Multiple Shear Springs Algebraic Model can simulate, with smooth transitions, the response of FRBs under small and large displacement amplitudes. In particular, the model can simulate the typical softening behavior displayed by these bearings under large displacements. Using this model, only one set of five parameters is needed to initiate the analyses. These parameters can be determined from cyclic experimental tests on the bearings. Results of the proposed hysteretic model are compared to experimental results obtained via bidirectional shake table tests. A good agreement between the experimental and the simulated results is obtained, confirming that the proposed model can be effectively used to predict the response of base-isolated buildings when softening of the bearings is expected under large deformations. Results of the analyses show that the proposed hysteresis model is capable of capturing the response of a building on FRBs with a good level of accuracy.

Keywords: Fiber-reinforced elastomeric bearing; Biaxial model; Response History Analyses

1. Introduction

Elastomeric bearings have been commonly used for base isolation applications in bridge and buildings. These bearings are made by bonding together thin layers of reinforcement and layers of rubber [1,2]. Two types of elastomeric bearings are available: Steel Reinforced Elastomeric Bearings (SREBs or SRBs) and Fiber Reinforced Elastomeric Bearings (FREBs of FRBs). While SRBs are generally rigidly connected to the upper and the lower structure [2], no bonding is required when adopting FRBs in base isolation applications [3].

This study focuses on a low-cost BI system which has proved to be effective in protecting buildings and their contents under severe ground motion excitations: the Recycled Rubber - Fiber Reinforced Bearings (RR-FRBs). These devices are made by gluing together, using a polyurethane adhesive, layers of a fabric reinforcement and layers of recycled rubber. The recycled rubber is obtained from scrap tires and industrial leftovers. Details of the production technology and material properties of the recycled rubber used for the manufacturing of these bearings are discussed in a research work by Montella et al. [4].

The application of RR-FRBs to a scaled building and results of shaking table tests have shown that a good earthquake response can be obtained thanks to the application of these bearings [5]. Because of a fabric reinforcement is used for the manufacturing of the bearings, each device can be obtained by cutting a pad of a large size. Also, the elastomeric material used for the production of RR-FRBs is low cost and eco-friendly. Because of the simple manufacturing process of RR-FRBs, these bearings are very low-cost if compared to conventional devices for structural control.

2. Tested Fiber-Reinforced Elastomeric Bearings

The tests here discussed were performed on square bearings of 70x70mm. These RR-FRBs (See Figure 1) consisted of 12 layers of recycled rubber bonded to 11 layers of 2-dimensional carbon fiber fabric. The recycled rubber for the manufacturing of these bearings shows a secant shear modulus G at 50% shear strain of 1.1 MPa and an equivalent viscous damping of approximately 10-15%. The cycles of hysteresis used for this research, were obtained during a large experimental program on RR-FRBs, results of which have been published in many research works (*e.g.* [6, 7]).

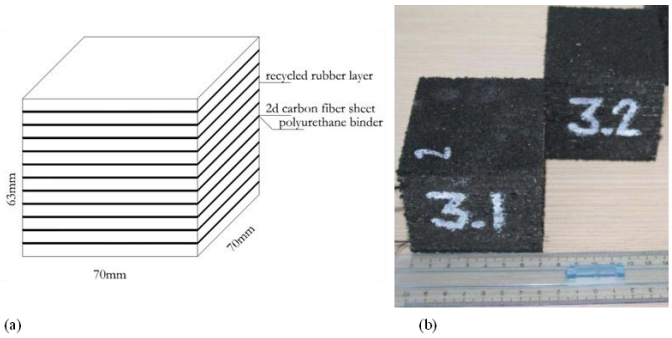

Fig. 1 – a) Schematic of the tested RR-FRBs, b) Picture of the tested devices [6].

The quasi-static response of the bearings under displacements of increasing magnitude has been discussed in Kelly and Calabrese [8]: when the lateral displacement increases, the bearings start to roll-off from the supports and their peak lateral resisting capacity is reached for a displacement of approximately half of the base of the bearings. For larger displacements, the bearings show a softening response up to the complete roll-over.

The hysteresis response of the 70x70mm RR-FRBs here discussed is given in Figure 2. As clear from the plot, for low amplitudes of deformation, the response of the bearings is almost linear, showing a low level of energy dissipation (i.e., damping). When the lateral displacement increases, the backbone of the hysteresis loops shows a softening response due to instability of the bearings under large displacement

magnitudes. For a large deformation, the effective stiffness of the bearings is reduced, while the equivalent viscous damping increases. As discussed in the work by Spizzuoco at al. [6], the tested bearings showed an effective stiffness of 225 N/mm and equivalent viscous damping of 13.5 for a shear strain of 15%. The effective stiffness reduced to a value of 80 N/mm, while the equivalent viscous damping increased to a value of 30% for a shear strain of 50%.

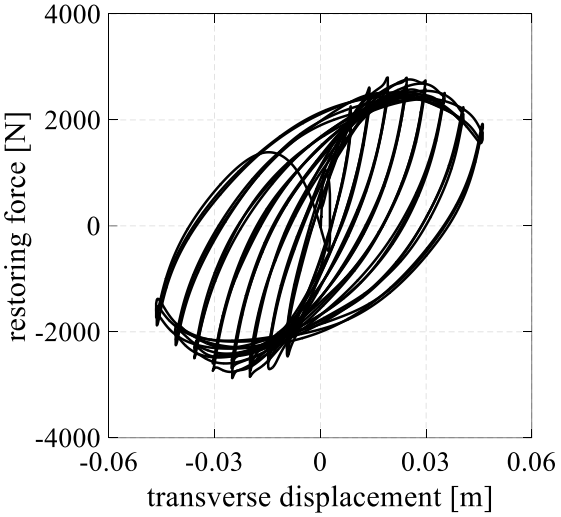

Fig. 2 – Hysteretic response of the 70x70mm RR-FRBs [5].

3. Proposed Multiple Shear Springs Algebraic Model

In this section, we present a novel multiple shear springs model able to simulate the transverse bidirectional behavior displayed by the seismic isolation devices described in Section 2. Such a hysteretic model requires only 5 parameters that can be easily obtained by fitting the experimental results. These variables are k_a, k_b, α, β_1 and β_2. The novel model is denominated Multiple Shear Springs Algebraic Model because it sees a combination of the multiple shear springs model, originally proposed by Wade and Hirose [9], and of the algebraic model developed by Vaiana et. al [10, 11] (which belongs to a more general family of uniaxial hysteretic models [12]).

3.1 General Formulation

In the proposed model, the bearing restoring forces along two transverse orthogonal directions, namely *x* and *y*, are evaluated as follows:

$$f_x = \sum_{i=0}^{n} f^{(i)} \cos \varphi^{(i)}, \qquad f_y = \sum_{i=0}^{n} f^{(i)} \sin \varphi^{(i)} \tag{1}$$

where $f^{(i)}$ represents the force of the *i*-th spring, $\varphi^{(i)}$ is the angle between the *i*-th spring and the *x* direction, whereas *n* is the total number of adopted springs. The *i*-th spring displacement, required to compute the force $f^{(i)}$, is obtained as:

$$u^{(i)} = u_x \cos\varphi^{(i)} + u_y \sin\varphi^{(i)} \tag{2}$$

where u_x and u_y are, respectively, the bearing displacements along the *x* and *y* transverse directions.

In the following subsections, we present the expressions of the *i*-th spring force $f^{(i)}$ and history variable $u_j^{(i)}$, as well as the expressions of the *i*-th spring internal parameters, namely $u_0^{(i)}$ and $f_0^{(i)}$. Over the coming sections, in order to simplify the notation, the superscript (*i*) will be omitted.

3.2 Expression of the *i*-th Spring Force

The *i*-th spring force, during the generic loading case, is derived solving the equation:

$$f\left(u,\, u_j^+\right) = \begin{cases} c^+\left(u,\, u_j^+\right) & u \in \left[u_j^+ - 2u_0,\, u_j^+\right] \\ c_u\left(u\right) & u \in \left[u_j^+,\, \infty\right) \end{cases}, \tag{3}$$

which, during the generic unloading case, becomes:

$$f\left(u,\, u_j^-\right) = \begin{cases} c^-\left(u,\, u_j^-\right) & u \in \left[u_j^-,\, u_j^- + 2u_0\right] \\ c_l\left(u\right) & u \in \left(-\infty,\, u_j^-\right] \end{cases}. \tag{4}$$

In the previous equations, c^+ and c^- represent, respectively, the *i*-th spring generic loading and unloading curves, evaluated as:

$$\begin{aligned} c^+\left(u,\, u_j^+\right) &= \beta_1 u^3 + \beta_2 u^5 + k_b u + \left(k_a - k_b\right)\left[\frac{\left(1+u-u_j^+ + 2u_0\right)^{(1-\alpha)}}{1-\alpha} - \frac{\left(1+2u_0\right)^{(1-\alpha)}}{1-\alpha}\right] + f_0, \\ c^-\left(u,\, u_j^-\right) &= \beta_1 u^3 + \beta_2 u^5 + k_b u + \left(k_a - k_b\right)\left[\frac{\left(1-u+u_j^- + 2u_0\right)^{(1-\alpha)}}{\alpha-1} - \frac{\left(1+2u_0\right)^{(1-\alpha)}}{\alpha-1}\right] - f_0 \end{aligned} \tag{5}$$

whereas c_u and c_l are, respectively, the *i*-th spring upper and lower limiting curves, computed as:

$$\begin{aligned} c_u\left(u\right) &= \beta_1 u^3 + \beta_2 u^5 + k_b u + f_0, \\ c_l\left(u\right) &= \beta_1 u^3 + \beta_2 u^5 + k_b u - f_0. \end{aligned} \tag{6}$$

3.3 Expression of the *i*-th Spring History Variable

The expression of the *i*-th spring history variable u_j^+, during the generic loading case, is:

$$u_j^+ = 1 + u_P + 2u_0 - \left\{\frac{1-\alpha}{k_a - k_b}\left[f_P - \beta_1 u_P^3 - \beta_2 u_P^5 - k_b u_P - f_0 + \left(k_a - k_b\right)\frac{\left(1+2u_0\right)^{(1-\alpha)}}{1-\alpha}\right]\right\}^{\left(\frac{1}{1-\alpha}\right)}, \tag{7}$$

whereas, the expression of the history variable u_j^-, during the generic unloading case, is:

$$u_j^- = -1 + u_P - 2u_0 + \left\{ \frac{\alpha - 1}{k_a - k_b} \left[f_P - \beta_1 u_P^3 - \beta_2 u_P^5 - k_b u_P + f_0 + (k_a - k_b) \frac{(1+2u_0)^{(1-\alpha)}}{\alpha - 1} \right] \right\}^{\left(\frac{1}{1-\alpha}\right)}, \quad (8)$$

where u_P and f_P are the coordinates of the starting point of the generic loading or unloading curve.

3.4 Expression of the *i*-th Spring Internal Parameters

The *i*-th spring internal parameters f_0 and u_0 are expressed in terms of the *i*-th spring parameters k_a, k_b, and α. Specifically, the expression of f_0 is:

$$f_0 = \frac{k_a - k_b}{2} \left[\frac{(1+2u_0)^{(1-\alpha)} - 1}{1-\alpha} \right], \quad (9)$$

whereas, the expression of u_0 is:

$$u_0 = \frac{1}{2} \left[\left(\frac{k_a - k_b}{10^{-8}} \right)^{\frac{1}{\alpha}} - 1 \right]. \quad (10)$$

4. Experimental Verification

This section discusses the findings of the analyses of a base isolated steel frame under bi-directional seismic excitation. The numerical results were obtained by implementing the multiple shear springs algebraic model to define the restoring force in each of the base isolation devices of the structure.

4.1 Base-Isolated Structure Properties

A detailed description of the experimental setup, test protocol and results of the shaking table tests are given in Losanno et al. [5]. Figure 3 shows a view of the three-dimensional (3D) computer model used in this study to simulate the response of the base isolated building on RR-FRBs. The structural model consists of a base isolation layer and an upper structure. The geometry of the model is defined in a global, right-handed Cartesian coordinate system, denoted with *X*, *Y*, and *Z*. The center of the reference system was located at the center of the mass of the base isolation layer. The superstructure has plan dimensions of 2.0 m (*X*-axis) by 2.5 m (*Y*-axis). The story height is 3.04 m. The mass of the superstructure is 4155 kg, while the mass of the base isolation system is 3545 kg. When fixed at the base, the first three periods of vibration of the upper structure are T_{s1} = 0.271 s, T_{s2} = 0.271 s, and T_{s3} = 0.156 s, respectively.

Four RR-FRBs (described in Section 2), one under each column, constitute the base isolation system of the structure. Above the base isolation layer, the diaphragm is rigid. The structural model for the analyses was based on the following assumptions: (i) the superstructure is linear; (ii) diaphragms are rigid; (iii) frames are axially inextensible; (iv) beams are rigid in bending; and (iv) the seismic isolators are rigid in compression. As a result of these assumptions, the total number of degrees of freedom of the base isolation layer is 3 (i.e., translation in *X* and *Y*, rotation about the *Z* axis).

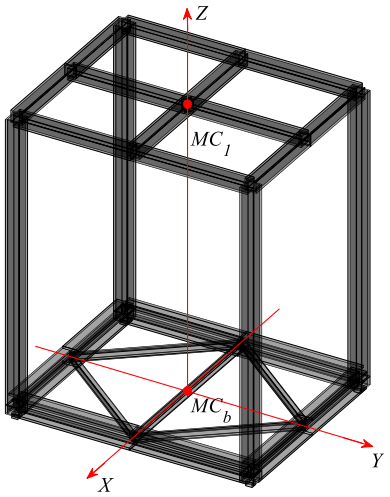

Fig. 3 – (a) 3D structural model of the base-isolated structure, (b) small scale building on RR-FRBs tested at the University of Naples [7].

4.2 Ground Motions

Results of the experimental and the numerical analyses here described are given for the 2003 Bingol ground motion (*X* and *Y* components). Figures 4a and 4b show the time history of the ground acceleration in both the *X* and *Y* directions. A scale factor of 30% along *X* and of 100% along *Y* was used for the analyses.

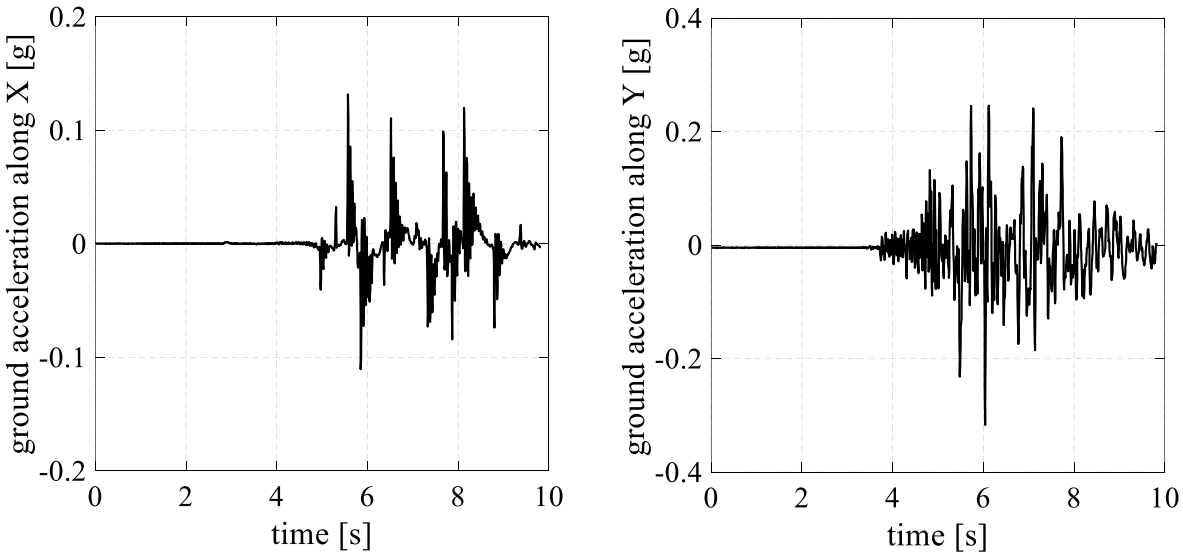

Fig. 4 – 2003 Bingol ground acceleration along the (a) *X* and (b) *Y* directions.

4.3 Hysteretic Model Parameters and Solution Algorithm

The hysteretic behavior of each unbonded fiber-reinforced elastomeric bearing is simulated by adopting the proposed multiple shear springs algebraic model, presented in Section 3. In particular, the total number of adopted springs is $n = 18$, whereas the model parameters of the i-th spring are listed in Table 1.

For the numerical integration of the nonlinear equilibrium equations of the 3D structural model, an explicit structure-dependent time integration method belonging to the Chang's family of explicit methods [13] is employed [11]. This algorithm is one of the most computationally efficient time integration methods available for the Response History Analyses (RHAs) of seismically base-isolated structures (Nagarajaiah et al. [14], Greco et al. [15]).

The hysteretic model and the solution algorithm have been programmed in MATLAB and run on a computer having an Intel®Core™i7-4700MQ processor and a CPU at 2.40 GHz with 16 GB of RAM.

Table 1 – Parameters of the *i*-th spring adopted to perform the RHA.

k_a $\left[\text{Nm}^{-1}\right]$	k_b $\left[\text{Nm}^{-1}\right]$	α	β_1 $\left[\text{Nm}^{-3}\right]$	β_2 $\left[\text{Nm}^{-5}\right]$
78000	30000	250	0	0

4.4 Comparison Between Experimental and Numerical Responses

In this last subsection, the time histories of the numerical and the experimental response of the base-isolated structure are compared. Figure 5a and 5b show the comparison of the experimental and the simulated time histories of the relative displacement of the mass center (MC_b) along the *X* and the *Y* directions.

Figure 6a and 6b are a comparison of the experimental and the simulated time histories of the absolute acceleration of the center of the mass of the superstructure $\left(MC_1\right)$ along the *X* and the *Y* directions.

Generally speaking, the results of the numerical analyses are in good agreement with the experimental findings.

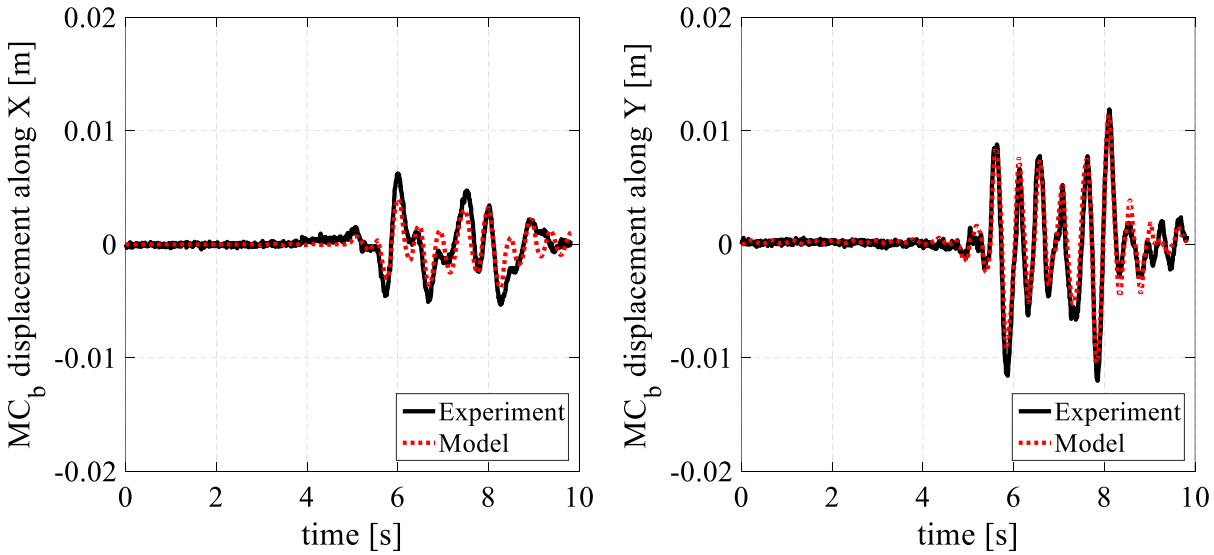

Fig. 5 – MC_b relative displacement time histories along the (a) *X* and (b) *Y* directions.

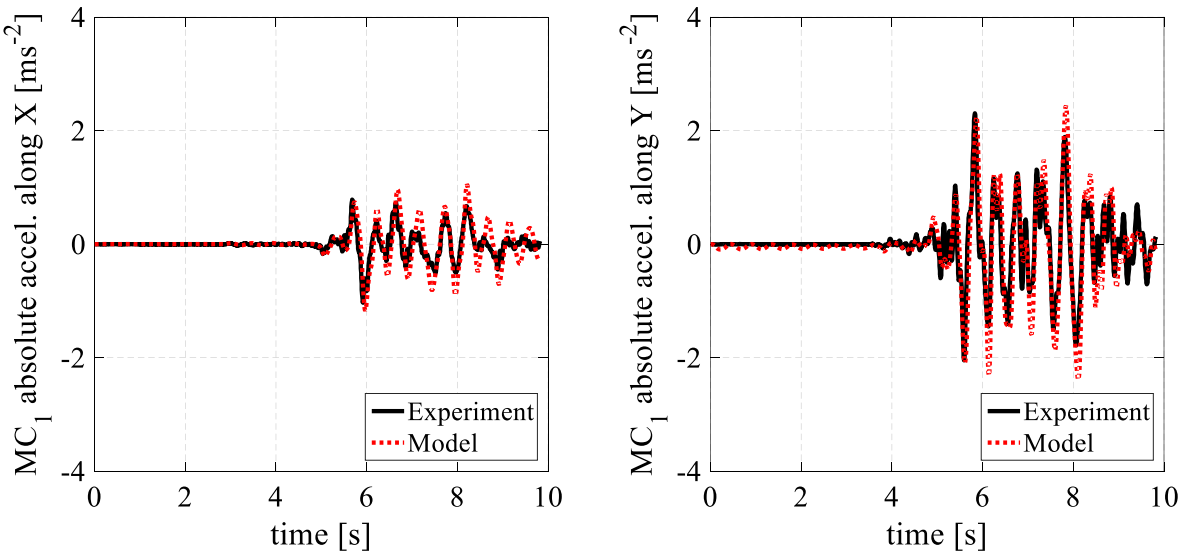

Fig. 6 – MC_1 absolute acceleration time histories along the (a) *X* and (b) *Y* directions.

5. Conclusions

This research work describes the extension of a uniaxial hysteresis model developed by Vaiana [12] to 2D by using the multi-spring approach. In the first part of this work, coefficients for the algebraic model were derived starting from available results of 1D tests on a novel type of base isolation devices. Based on the parameters obtained by fitting the numerical response to the measured hysteresis cycles, response history analyses where run to predict the response of a scaled building on RR-FRBs under ground motion excitation.

Results of the analyses were found to predict, with a good level of accuracy, the response of a building on RR-FRBs in terms of displacement and acceleration histories. While these initial results are encouraging, addition effort has to be dedicated to assess the results and the efficiency of the proposed model against those of model of hysteresis already available in literature (*e.g.*, Bouc-Wen [16-18], Kikuchi and Aiken [19]).

6. References

[1] Kelly, J.M., (1999): Analysis of Fiber-Reinforced Elastomeric Isolators. *Journal of Seismology and Earthquake Engineering*, **2** (1), 19-34

[2] Kelly, J.M., (2002): Seismic isolation systems for developing countries. *Earthquake Spectra*, **18** (3), pp.385-406.

[3] Nanda, R.P., Shrikhande, M. and Agarwal, P., (2015): Low-cost base-isolation system for seismic protection of rural buildings. *Practice Periodical on Structural Design and Construction*, **21** (1), p.04015001.

[4] Montella, G., Calabrese, A. and Serino, G., (2014): Mechanical characterization of a Tire Derived Material: Experiments, hyperelastic modeling and numerical validation. *Construction and Building Materials*, **66**, pp.336-347.

[5] Losanno, D., Spizzuoco, M. and Calabrese, A., (2019): Bidirectional shaking‐table tests of unbonded recycled‐rubber fiber‐reinforced bearings (RR‐FRBs). *Structural Control and Health Monitoring*, **26** (9), p.e2386.

[6] Spizzuoco, M., Calabrese, A. and Serino, G., (2014): Innovative low-cost recycled rubber–fiber reinforced isolator: experimental tests and finite element analyses. *Engineering Structures*, **76**, pp.99-111.

[7] Calabrese, A., Spizzuoco, M., Serino, G., Della Corte, G. and Maddaloni, G., (2015): Shaking table investigation of a novel, low‐cost, base isolation technology using recycled rubber. *Structural Control and Health Monitoring*, **22** (1), pp.107-122.

[8] Kelly, J.M. and Calabrese, A., (2012): Mechanics of fiber reinforced bearings. *Technical Report PEER 2012/101*, Pacific Earthquake Engineering Research, Berkeley, USA

[9] Wada A, Hirose K (1989) Elasto-plastic dynamic behaviors of the building frames subjected to bi-directional earthquake motion. *Journal of Structural and Construction Engineering* (Transactions of AIJ) **399**: 37-47 (in Japanese).

[10] Vaiana N, Sessa S, Marmo F, Rosati L (2019): An accurate and computationally efficient uniaxial phenomenological model for steel and fiber reinforced elastomeric bearings. *Composite Structures*, **211**, pp.196-212.

[11] Vaiana N, Sessa S, Marmo F, Rosati L (2019): Nonlinear dynamic analysis of hysteretic mechanical systems by combining a novel rate-independent model and an explicit time integration method. *Nonlinear Dynamics*, **98** (4): pp.2879-2901.

[12] Vaiana N, Sessa S, Marmo F, Rosati L (2018): A class of uniaxial phenomenological models for simulating hysteretic phenomena in rate-independent mechanical systems and materials. *Nonlinear Dynamics*, **93** (3), pp.1647-1669.

[13] Chang S-Y (2014): Family of structure-dependent explicit methods for structural dynamics. Journal of Engineering Mechanics, ASCE 140(6): 1-7.

[14] Nagarajaiah S, Reinhorn AM, Constantinou MC (1991): Nonlinear dynamic analysis of 3-D base-isolated structures. *Journal of Structural Engineering*, ASCE **117** (7), pp.2035-2054.

[15] Greco F, Luciano R, Serino G, Vaiana N (2018): A mixed explicit-implicit time integration approach for nonlinear analysis of base-isolated structures. *Annals of Solid and Structural Mechanics*, **10** (1-2), pp.17-29

[16] Bouc, R. (1971): Modele mathematique d'hysteresis. *Acustica*, **24**, pp.16–25

[17] Wen,Y. (1976): Method for random vibration of hysteretic systems. *J. Eng. Mech. Divis. ASCE*, **102** (2), pp.249–263

[18] Wen, Y. (1980): Equivalent linearization for hysteretic systems under random excitation. *J. Appl.Mech. ASME* **47** (1), pp.150– 154

[19] M. Kikuchi, I.D. Aiken, A. Kasalanti (2012): Simulation analysis for the ultimate behavior of full-scale lead-rubber seismic isolation bearings. *15th World Conference on Earthquake Engineering*, Lisbon, Portugal.

